













The predicted QPM wavelengths for these processes match quite well the spectral locations of the dips seen in the spectrum of Fig. 3a, at  $\lambda_s = 1515$  nm (2nd order QPM for pump-idler SFG, with  $\Lambda = 25$   $\mu\text{m}$ ) and  $\lambda_s = 1406$  nm (3rd order QPM for pump-signal SFG). Similar calculations done for  $\Lambda = 26$   $\mu\text{m}$  predict declines in intensity at 1580 nm and at 1405 nm, consistent with the experimental observations (Fig. 3b).

The span of the OSA measurement in Fig. 3a covers also the degeneracy wavelength,  $\lambda_{s,i} = 1720$  nm (indicated by the red mark), and it can be noticed that the intensities are not symmetric around the degeneracy point. Instead they appear to monotonically decrease on the longer wavelength side. As a matter of fact, such a decaying trend at the edge of the OSA spectral range appears to be an artefact of the instrument, as confirmed by the sets of measurements that we subsequently performed on the OPG output with the spectrometer. With the latter we could also directly measure the full OPG bandwidths, covering both the signal and idler spectral ranges.

One such measurement, corrected for the absorption of the optical elements between the PPMg:SLT sample and the detector, is shown in Fig. 4, where we plot the experimental data (solid blue curve) recorded at the same working point as the one of Fig. 3a ( $\Lambda = 25$   $\mu\text{m}$ ,  $\lambda_p = 860$  nm). From Fig. 4 it is apparent that there is no real decrease in powers beyond the degeneracy point (indicated by the red mark).

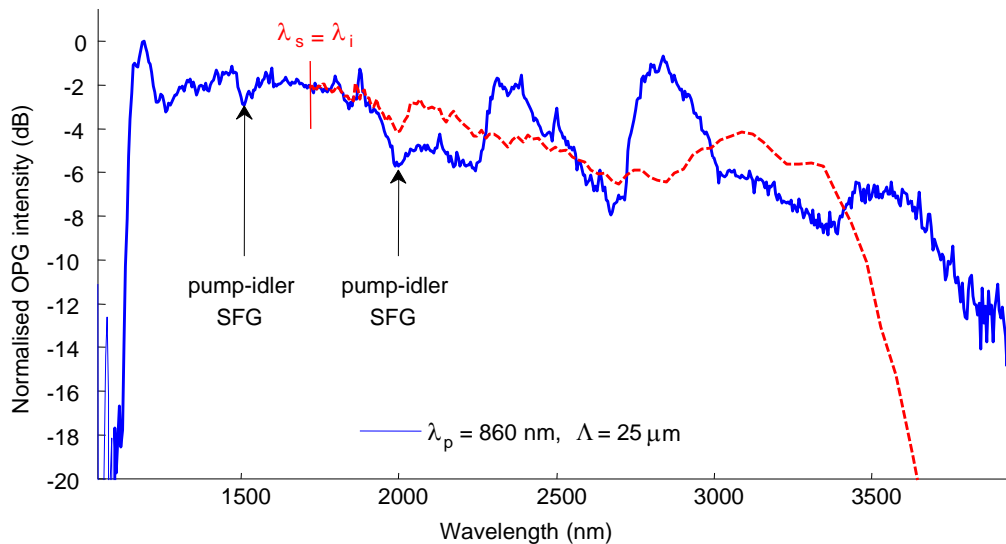


Fig. 4. Full OPG spectra from 1 mol% PPMg:SLT at  $T = 80^\circ\text{C}$ , generated with 25  $\mu\text{m}$  period using a pump beam of 860 nm, 78 mW power and 2.7 ps pulse duration focused to 100  $\mu\text{m}$  radius. The dashed red line represents a prediction of the idler intensities, calculated from the detected signal intensities. The integration time of the PbSe detector used with the Horiba Jobin Yvon monochromator was 900 ms.

To distinguish the contribution of OPG from that of other parametric processes observed on the long-wavelength side of the experimental data, in Fig. 4 we plot a prediction of the idler spectrum (red dashed curve). It is calculated from the signal intensities ( $\lambda_s < 2\lambda_p$ ) by using the Manley-Rowe relations:  $P_s/\omega_s = P_i/\omega_i = -P_p/\omega_p$ , where  $P_x$  and  $\omega_x$  are the power and frequency, respectively, of the interacting waves.

By comparing this prediction with the measurement we can identify three features in the idler spectrum which do not seem to be arising directly from the OPG process, namely the three broad peaks located at  $\lambda_i = 2.4, 2.8, 3.5$   $\mu\text{m}$ . The nature of those additional contributions to the PPMg:SLT output is the subject of current investigations. Their spectral locations match fairly well the expected positions for the 6th, 5th and 4th harmonics of a polariton wave

at 20 THz [21], which would strongly support their interpretation as the outcome of a concurrent stimulated Raman scattering process occurring in the sample.

A conservative estimate for the spectral extent of OPG in Fig. 4, based on the Manley-Rowe prediction for the longer-wavelength edge of the spectrum (neglecting the even broader tail seen in the experiments), indicates a bandwidth spanning more than one octave. The bandwidth at 10 dB is 180 THz, which is, to the best of our knowledge, the broadest band achieved so far in collinear parametric down-conversion.

In the spectrum of Fig. 4 we also pointed out spectral features associated to cascaded SFG processes (already discussed with reference to the spectra in Fig. 3) occurring in the sample. The signatures of pump-idler SFG, achieved by 2nd order QPM, can be discerned among the idler wavelengths at 2  $\mu\text{m}$  and at the corresponding signal wavelength of 1510 nm. On the other hand, pump-signal SFG does not seem to notably affect the spectrum.

As a final remark on the measurements of Fig. 4, the total energy content of the detected OPG pulses was 2  $\mu\text{J}$  for an input energy of 78  $\mu\text{J}$  (the threshold was  $\sim 1$   $\mu\text{J}$ ). The maximum fluctuations observed in the OPG output energy (monitored with a Newport germanium 918D-IR-OD3 photodetector) over a time of 5 minutes, noted for all the measurements of Figs. 3 and 4, amounted to  $\Delta\mathcal{E}/\mathcal{E} = 7\%$ . Preliminary measurements of the OPG response as a function of pump energy, for the conditions of Fig. 4, show that a linear regime prevails up to  $\sim 20$   $\mu\text{J}$ , with a slope conversion efficiency of 6%. Saturation effects appearing at higher pump energies reduce the conversion efficiency to 3% at the highest investigated pump energy. The OPG energy can be further increased by realising an OPA scheme following the OPG stage. In addition, the low coercive field of Mg:SLT allows for thicker crystals to be periodically poled, which could enable further scaling to higher powers.

## 5. Conclusion

We have reported on ultra-broadband parametric gain in periodically poled Mg:SLT, pumped with picosecond pulses in the vicinity of the zero GVD point of the material. OPG bandwidths as broad as 180 THz (at 10 dB), spanning the full spectrum from 1.1 to 3.5  $\mu\text{m}$ , were achieved with a pump at 860 nm in PPMg:SLT with 25  $\mu\text{m}$  poling periods. This is to the best of our knowledge the broadest band observed in collinear parametric down-conversion to date. When compared to previous results in PPLN and PPKTP, OPG in PPMg:SLT exhibited also a remarkable spectral flatness.

The combination of extremely broad bandwidths and high parametric gain [16] affordable in PPMg:SLT makes this material a promising candidate for applications to high-power, ultra-short pulse generation and amplification. Given the optimum pump wavelength of 860 nm, it is interesting to consider broadband parametric systems pumped by Cr:LiSAF lasers and amplifiers, which can be directly diode pumped and can also generate large pulse energies at this wavelength [22].

## Acknowledgements

This work was partially supported by the Linnaeus Centre ADOPT, the Swedish Research council (Vetenskapsrådet), the Knut and Alice Wallenberg Foundation, and the EU 7th Framework Programme. K. G. Also gratefully acknowledges support from the European Commission through a Marie Curie grant (PIEF-GA-2009-234798).